ELSEVIER

Chemical Engineering Science 60 (2005) 347–363

Chemical Engineering Science

www.elsevier.com/locate/ces

Multiobjective optimization of an industrial styrene monomer manufacturing process

A. Tarafder, G.P. Rangaiah, Ajay K. Ray*

Department of Chemical and Biomolecular Engineering, National University of Singapore, 10 Kent Ridge Crescent, Singapore 119260, Singapore

Received 6 February 2004; received in revised form 6 July 2004; accepted 27 July 2004
Available online 30 September 2004

Abstract

Multi-objective optimization of the operation and design of a styrene manufacturing process has been studied with the elitist non-dominated sorting genetic algorithm (NSGA-II). In the first part, the study focused on bi-objective optimization and comparative analysis of three different styrene reactor designs—the single-bed, the steam-injected and the double-bed reactors. The objectives were to simultaneously maximize styrene flow rate and styrene selectivity. In the second part, on the other hand, a tri-objective optimization study was performed involving the entire manufacturing process consisting of the reactor, heat-exchangers and separation units. Only the double-bed reactor was considered in this study for maximizing the styrene flow rate and selectivity and minimizing the total heat duty required by the manufacturing process. Results are presented and discussed in detail.

Keywords: Styrene; Modelling; Simulation; Multiobjective; Optimization; Pareto set; NSGA; Chemical reactors; Process systems engineering; Reaction engineering; Industrial process

1. Introduction

Styrene is one of the most manufactured monomer in the world with an annual turnover of 60 billion USD [www.styreneforum.org] comprising thousands of companies and facilities. It is the raw material for the production of polystyrene, acrylonitrile–butadiene–styrene resins (ABS) and a variety of miscellaneous polymers, which are the basic materials of the plastic revolution. Surely, even a small improvement in the plant operation will have a significant impact on the revenue of the industries, which in turn will benefit the consumers as well.

In a continuing effort to improve the performance of styrene manufacturing process, researchers have carried out several modelling and optimization studies for the last few decades with the latest analytical tools available. An account of these studies is available in our recent publication (Yee et al., 2003), where an effort was made to optimize a styrene reactor unit, maximizing the styrene flow, yield and selectivity, using a genetic algorithm, the non-dominated sorting genetic algorithm (NSGA) (Srinivas and Deb, 1995), developed for multi-objective optimization. Encouraged by the outcome of this effort, we have carried out an optimization study on a styrene manufacturing process, with a more recent algorithm—the elitist non-dominated sorting genetic algorithm or NSGA-II (Deb et al., 2002). Although NSGA was successfully applied to many multi-objective optimization problems (Yee et al., 2003; Rajesh et al., 2001; Bhaskar et al., 2000), Deb et al. (2002) reported that its computational complexity can be drastically reduced and by applying elitism, a method of preserving good solutions, its performance can be still increased. This revision in NSGA resulted in NSGA-II which was shown to be able to achieve better convergence near the true Pareto-optimal front and find much better spread of Pareto-optimal solutions (Deb et al., 2002). Recent publications (Kasat and Gupta, 2003; Mitra and Gopinath, 2004) which used NSGA-II, as well as

* Corresponding author. Tel.: +65-6874-8049; fax: +65-6779-1936.
E-mail address: cheakr@nus.edu.sg (A.K. Ray).

0009-2509/$ - see front matter © 2004 Elsevier Ltd. All rights reserved.
doi:10.1016/j.ces.2004.07.120

our experience with both NSGA and NSGA-II, endorse the claim of Deb et al.

The styrene manufacturing process, used in the current optimization study, contains styrene monomer reactor along with heat-exchangers and separation units. Reactors with three different designs have been used for the study, with the goal of maximizing styrene flow rate and selectivity and minimizing the overall heat duty required by the manufacturing process. The next section contains a detailed description of the process.

2. Process description

Fig. 1 shows the schematic diagram of a typical styrene monomer (SM) manufacturing process consisting of a reactor unit, where dehydrogenation of ethylbenzene (EB) takes place, followed by reactor effluent cooling units (HE1, HE2 and PC) and separation units (S1–S3), where the SM is separated from un-reacted EB and other by-products. The reaction is carried out in vapour phase with steam, over a catalyst consisting primarily of iron oxide. Fresh EB feed (F^0_{EB} at T^0_{EB}) and recycled EB are mixed with low pressure saturated steam ($\alpha F^0_{\mathrm{stm}}$ at T^0_{stm}) in a mixer and preheated to a temperature of T_{C2} with reactor effluent in HE1. This stream is further heated up to the reaction temperature, generally over 875 K (Clough and Ramirez, 1976), by superheated steam from a fired heater before being passed into the fixed bed catalytic reactor. In most of the modern plant designs (see Fig. 2), the reactor unit consists of two or three reactors in series (Lee and Hubbell, 1982), which is to provide reheating to the reactants (as the main reaction is endothermic) and hence boosting forward reaction. The most popular method of adding heat is to indirectly warm up the reactants between the beds, although, in some other plant designs, steam is directly injected at the entrances of the reactor beds to provide reheat for the subsequent section(s). Although steam is added mainly to provide the heat of reaction, there are other reasons for its use; a detailed discussion of which can be found in our previous publication (Yee et al., 2003). Usually, a steam to EB ratio (SOR) of 15:1 is maintained at the reactor inlet.

The six main reactions occurring in the styrene reactor are (Sheel and Crowe, 1969):

$$C_6H_5CH_2CH_3 \leftrightarrow C_6H_5CHCH_2 + H_2, \quad (1)$$

$$C_6H_5CH_2CH_3 \rightarrow C_6H_6 + C_2H_4, \quad (2)$$

$$C_6H_5CH_2CH_3 \rightarrow C_6H_5CH_3 + CH_4, \quad (3)$$

$$2H_2O + C_2H_4 \rightarrow 2CO + 4H_2, \quad (4)$$

$$H_2O + CH_4 \rightarrow CO + 3H_2, \quad (5)$$

$$H_2O + CO \rightarrow CO_2 + H_2. \quad (6)$$

The main reaction in the styrene reactor is the reversible, endothermic conversion of EB to styrene and hydrogen (Eq. (1)). This reaction proceeds thermally with low yield and catalytically with high yield. As it is a reversible reaction, producing two moles of product to one mole of reactant, low pressure and high temperature favour the forward reaction (Le Chatellier's principle). Although the dehydrogenation of EB is both kinetically and thermodynamically favoured by high temperature, by-products like benzene and toluene are produced by thermal cracking at higher temperatures (Eqs. (2) and (3)), reducing the styrene selectivity. Hence, operating temperature should be chosen compromising between the conversion of EB and styrene selectivity. In addition, special catalyst is used to promote higher production of

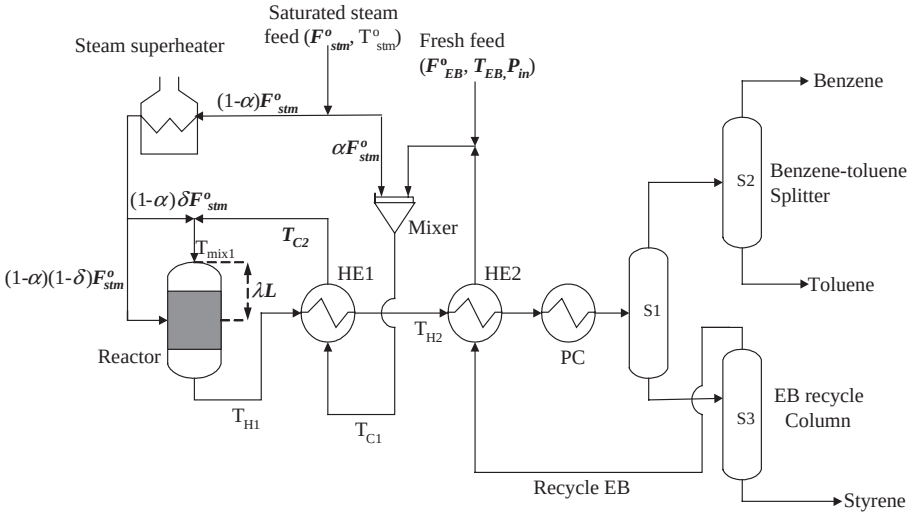

Fig. 1. Schematic diagram of Styrene plant. (HE: heat-exchanger, S: Separator, PC: partial condenser). Letters in **bold** and *italics* represent decision variables.

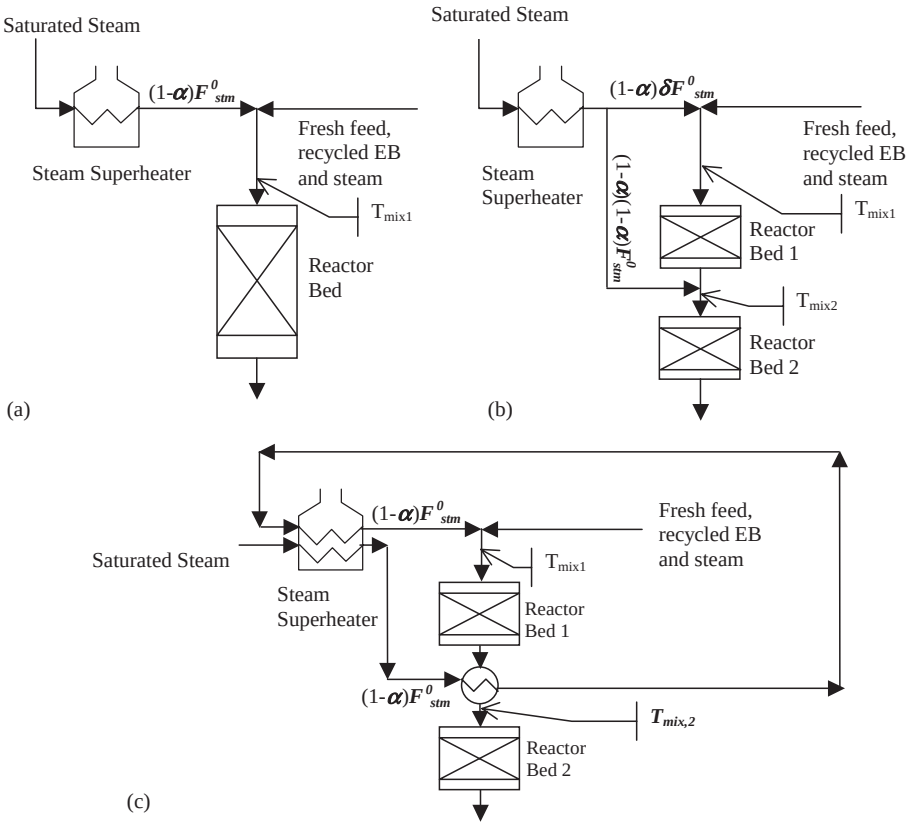

Fig. 2. Schematic diagram of (a) Single Bed (SB) reactor, (b) Steam-injected (SI) reactor and (c) Double Bed (DB) reactor. Letters in **bold** and *italics* represent decision variables.

styrene at lower temperature while minimizing the side reactions.

The effluent from the reactor unit is cooled in the cooling section consisting of heat exchangers (HE1 and HE2) and partial condenser (PC). The condensed, crude styrene, together with the main by-products (toluene and benzene) and un-reacted EB, separates from water and non-condensable gases like H_2 in a settling drum (not shown in the figure). The crude styrene is then taken to the distillation units (S1–S3) for the recovery of styrene. The purity requirement of styrene in industry is circa 99.7 wt%.

3. Mathematical modelling and simulation of the styrene plant

In the present study, a pseudo-homogeneous model suggested by Sheel and Crowe (1969) was used for styrene reactor. The model assumes lumped catalytic effects in the bulk fluid phase inside the reactor, so the mass and heat transfer within the catalyst pellet are assumed to be negligible. A detailed account of this model is available in our previous work (Yee et al., 2003) as well as other literature (Sheel and Crowe, 1969; Elnashaie and Elshishini, 1994).

In the present study, the same reactor model is used to simulate three different configurations of the styrene reactor unit, based on different EB and steam supply schemes to the reactor. The first one is the single bed (SB), where there is no intermediate heating and the entire superheated steam is mixed with the EB-steam mixture and injected at the reactor entrance (Fig. 2(a)). In the second configuration (Fig. 2(b)), only a portion of the total available superheated steam is mixed with the EB-steam mixture at the reactor entrance, whereas, the rest of the steam is injected at another suitable place. It will be called a steam-injected (SI) reactor and is modelled as two SB reactors in series, with a superheated steam flow, mixing directly with the effluent from the first part, before entering the second. The third and the last configuration (Fig. 2(c)), which is the most popular in the industries, is modelled as two SB reactors operating in series. Here, superheated steam flow, unlike the SI reactor, indirectly heats up the effluent from the first bed inside a heat exchanger. Subsequently, the steam is again superheated, taken to the reactor inlet, mixed with the EB-steam mixture and fed to the reactor.

3.1. Distillation columns

Other than the reactor system, the distillation columns that separate the unconverted EB from styrene is the most important and expensive equipment in a styrene plant. It is

Table 1
Specifications for the three columns

Column	Light key	Heavy key	f_{iD}[a]	f_{jB}[b]
Benzene–toluene Column	Toluene	Ethylbenzene	DV	DV
Benzene–toluene Splitter	Benzene	Toluene	0.999	0.999
Ethylbenzene recycle Column	Ethylbenzene	Styrene	DV	0.997

[a] f_{iD} is the fractional recovery of the light key in distillate.
[b] f_{jB} is the fractional recovery of the heavy key in bottoms.

expensive because close boiling points of EB and styrene require a large number of distillation stages (70–100) (Denis and Castor, 1992). As styrene is one of the few monomers that auto-polymerizes, the styrene purification has to be carried out in low temperature vacuum distillation columns to minimize polymerization. In this study, three distillation columns each operating at 0.1 bar are utilized, where the separation scheme is a simplified version of the standard scheme used in Fina/Badger process (Lee and Hubbell, 1982). The benzene and toluene are separated from EB and styrene in the first column, where the overhead, consisting of benzene and toluene, is sent to a benzene–toluene splitter to recover benzene and toluene. The bottoms stream, on the other hand, is sent to the EB recycle column, where EB is separated from styrene and recycled back to the dehydrogenation reactor.

The product distribution, actual number of theoretical stages, reflux ratio, condenser and reboiler duties are determined by employing shortcut methods, commonly known as Fenske–Underwood–Gilliland (FUG) method (Khoury, 1999). We have used the Molkanov's equation to represent the Gilliland correlation curve. The assumptions made to simplify the model were: (a) styrene, EB, benzene and toluene are the only components entering the distillation columns, (b) the solution is ideal, thus Dalton's law and Raoult's law are valid, (c) constant molar overflow and negligible pressure drop in the columns, (d) overall stage efficiency is 1.0, (e) the relative volatilities are constant throughout the columns, and (f) the columns use total condenser and partial reboiler.

The components in increasing order of volatility are styrene, EB, toluene and benzene. Based on the specifications of the key components and their recoveries shown in Table 1, the product distribution is determined. In Table 1, the DVs are the decision variables whose values are to be supplied by the optimizer (discussed in the next section). Based on the above assumptions and product distributions known, the column was modelled; the complete set of equations is available in related books (Khoury, 1999; Seider, 2004).

3.2. Heat exchangers

The effluent heat exchangers are an integral part of the styrene plant as they recover waste heat from the reactor effluent and heats up the EB feed, hence reducing the overall energy consumption. While modelling heat-exchangers for this study, only the energy balance equations were considered, as it was assumed that no chemical reactions are occurring inside, and the pressure-drops, to the fluid streams involved, are also negligible. The other assumptions made were (a) temperature varies only in axial direction, (b) heat transfer coefficient and flow rates of the hot and cold fluids are constant throughout the exchanger length, (c) no energy loss to the environment and heat gained by the cold stream is equal to heat lost by the hot stream, and (d) counter-current flow of fluids inside the heat exchanger. The governing equations are:

$$Q_{\text{cold}} = M\left(\left(\int_{T_{C1}}^{T_B} C_{p,L}\,\mathrm{d}T\right) + \Delta H_{\text{vap}} + \left(\int_{T_B}^{T_{C2}} C_{p,V}\,\mathrm{d}T\right)\right), \tag{7}$$

$$Q_{\text{hot}} = Q_{\text{cold}}, \tag{8}$$

$$m\int_{T_{H1}}^{T_{H2}} c_p\,\mathrm{d}T = Q_{\text{hot}}, \tag{9}$$

$$A = \frac{Q_{\text{cold}}}{U(\Delta T)_{\text{ln}}}. \tag{10}$$

For the present study the value of U was taken = 55 kJ/h/m^2/K (Saunders, 1988).

Two heat exchangers are used in the model, one for EB-steam pre-heater (HE1) and the other for recycled EB pre-heater (HE2). While HE1 considers no phase change occurring in any of its streams, HE2 considers a phase change in its cold fluid flow. The recycled EB from EB recycle column (S3) enters HE2 in a sub-cooled liquid state, reaches its boiling point inside HE2, and leaves as vapour having a temperature equal to the fresh EB inlet temperature T_{EB}. To determine the hot stream outlet temperature from Eq. (9), an iterative calculation was used using the subroutine DNEQNF of the IMSL FORTRAN library.

3.3. Partial condenser

The vapour entering the partial condenser is a multi-component mixture, consisting of non-condensable gases like, H_2, CO, CO_2, C_2H_4 and CH_4, steam condensate and water immiscible organic compounds, like C_6H_6, $C_6H_5CH_3$, $C_6H_5CHCH_2$ and $C_6H_5CH_2CH_3$. The exit temperature of condenser was set at 333 K in order to condense most of the steam and water-immiscible compounds. As pressure drop in heat exchangers was considered negligible, the pressure assigned to the condenser is equal to exit pressure of the reactor, which is usually less than 2 bar. It was assumed that the inlet mixture behaves ideally, obeying Dalton's law and Raoult's law since the vapour mixture is mostly steam (greater than 85% on a molar basis) and a low pressure is maintained inside the condenser. The solubility of non-condensable gases in the organic phase was also considered

negligible. Based on these assumptions, vapour–liquid equilibrium constant K for each component *i*, was defined as

$$K_i = \frac{y_i}{x_i} = \frac{P_i^{\text{sat}}}{P_{\text{cond}}} \tag{11}$$

and the moles of liquid condensed for each component i (L_i) is determined from

$$L = \sum L_i = \sum \frac{Y_i}{1 + K_i(V/L)}, \tag{12}$$

where Y_i is the original number of moles of component i in vapour, and V and L are the total moles of vapour remaining and the total moles of liquid formed respectively. To determine the amount of vapour condensed at the condenser temperature, first a value for (V/L) is assumed and the number of moles of liquid formed is calculated from Eq. (12). Subsequently, V is calculated from the difference of ($\sum Y_i$) and L, and if the new value of (V/L) ratio does not agree with its assumed value, another value is assumed and the iteration proceeds until convergence. With the amount of vapour condensed known, the sensible heat of vapour, sensible heat of liquid and latent heat of condensation for each component is calculated and the condenser duty is calculated as the summation of enthalpy changes for all the components.

4. Formulation of the optimization problem

The complete process of styrene production involves catalytic reaction, cooling and separation. Although all the steps are equally important, the catalytic conversion of EB to styrene is the most critical because at this step the ultimate styrene production, volume of by-products and volume of recycled EB to be handled—are all decided. Seeing the importance of the reactor unit, the present study has been divided into two parts—the first part studies only the reactor unit and the EB pre-heater (HE1), which is taken as it affects the reactor performance significantly. The second part, on the other hand, involves a study of the entire styrene production unit (see Fig. 1) including the styrene reactor, heat exchangers, condenser and separation columns.

As the purpose of operation is to produce styrene and it is the most costly product, the first objective of the optimization study was determined as maximization of styrene production. Added to that, minimization of the unwanted by-products, toluene and benzene, is also important as it causes raw material loss. To minimize the toluene and benzene production in the reactor, the selectivity of styrene should be increased. The above findings are summarized in the following equations, which are the objective functions for the first part of the present optimization study:

$$\text{Maximize}: \quad J_1 = F_{\text{st}}, \tag{13}$$

$$\text{Maximize}: \quad J_2 = S_{\text{st}} = \frac{F_{\text{st}} - F_{\text{st}}^0}{F_{\text{EB}}^0 - F_{\text{EB}}}. \tag{14}$$

Second part of the optimization study involves the entire manufacturing process (see Fig. 1). The main operating cost for the process, other than the raw material, involves water and the fuel to the steam boilers. Hence, while optimizing the entire styrene manufacturing process, the objective, which was included with the previous two, was minimization of the total heat duty. Heat duty minimization indirectly reduces the emission of gases e.g. CO_x, SO_x and NO_x to the environment, as well. These gases are produced in steam boiler by burning fuel and causes major environmental pollution.

$$\text{Minimize}: \quad J_3 = \Delta Q, \tag{15}$$

where ΔQ is the total heat duty, expressed in GJ/h, supplied as superheated and saturated steam flow to the reaction process as well as to the separation unit reboilers. Temperatures of saturated steam for initial heating-up of EB, superheated steam and steam used for the column reboilers are fixed at 405, 1025 and 373 K, respectively.

The optimization routine, real variable NSGA-II requires the objective functions to be described as minimization type. For maximizing J_1 and J_2 (Eqs. (13) and (14)), the actual objective functions were written as the following, which is one of the popular approaches for inversion (Deb, 2001),

$$I = \left[\frac{1}{1+J}\right]. \tag{16}$$

4.1. Decision variables and constraints

For the optimization of styrene plant, the decision variables were chosen from the operating variables of existing plants and from key design variables of the reactor (Sheel and Crowe, 1969; Elnashaie and Elshishini, 1994). For this study, the catalyst data were taken as fixed. The following decision variables and corresponding bounds were chosen for optimizing the styrene reactor–EB–pre-heater unit (see Fig. 1):

$$1.4 < P_{\text{in}} < 2.63\,\text{bar}, \tag{17}$$

$$7 < \text{SOR} < 20, \tag{18}$$

$$27.56 < F_{\text{EB}}^0 < 40.56\,\text{kmol/h}, \tag{19}$$

$$1.5 < D < 4.0\,\text{m}, \tag{20}$$

$$0.7 < L/D < 1.5, \ \text{dimensionless}, \tag{21}$$

$$450 < T_{\text{EB}} < 500\,\text{K}, \tag{22}$$

$$0.1 < \alpha < 1, \ \text{dimensionless}, \tag{23}$$

$$700 < T_{C2} < 900\,\text{K}, \tag{24}$$

Two additional decision variables for the SI type reactor (see Fig. 2) are:

$$0.1 < \lambda < 1, \ \text{dimensionless}, \tag{25}$$

$$0.1 < \delta < 1, \ \text{dimensionless}. \tag{26}$$

And, three additional decision variables for DB type reactor (see Fig. 2) are:

$$700 < T_{\text{mix2}} < 950\,\text{K}, \tag{27}$$

$$1.5 < D_2 < 4.0\,\text{m}, \tag{28}$$

$$0.7 < (L/D)_2 < 1.5, \text{ dimensionless.} \tag{29}$$

The lower and upper limits of the inlet pressure are taken as 1.4 and 2.63 bar, respectively, following the industrial practice. In this study, F^0_{EB} refers to the total pure EB feed and the bounds on the variable were determined as (−25%) and (+10%) of 36.87 kmol/h, the industrial value. The temperature of saturated steam is fixed at 405 K and the superheated steam temperature at 1025 K in view of limitations on materials of construction and electrical heaters in the superheater. The lower bound of the EB feed temperature, T_{EB} is selected as 450 K to ensure that the ethylbenzene is in the vapour phase. The lower limit of the steam-to-oil ratio, SOR is chosen as seven to prevent coke formation on the catalyst and therefore ensuring a longer catalyst lifespan. The upper limit of SOR is chosen as 20 as too high a SOR would be uneconomical due to the higher energy required for heating the excess steam to reaction temperature. Moreover, capacity limitations on downstream units like heat exchangers and condenser would have to be taken into consideration too.

EB conversion and styrene selectivity are affected by residence time. As residence time is a function of feed flow rate and reactor volume, F^0_{EB}, D and L/D are chosen as decision variables. As the diameter of the industrial reactor is 1.95 m (Sheel and Crowe, 1969), the lower and upper bounds of the diameter, D are set at 1.5 and 4 m to ensure that the size of the reactor is not too large or too small. The range for the length to diameter ratio (L/D) is 0.7 to 1.5, chosen consistent with industrial practice. Normally, 10% of the total saturated steam (F^0_{stm}) is mixed with ethylbenzene to prevent side reactions before ethylbenzene feed is injected into the reactor. Hence, steam fraction, α has been given a range of 0.1 to 1.0.

The lower bound of the EB pre-heater exit temperature, T_{C2} has been set at 700 K to provide sufficient heat of reaction. The upper bound is set at 900 K to ensure that T_{H1} is greater than T_{C2} for heat exchange between the streams. The two decision variables, δ and λ, determines the fraction of superheated steam fed to the SI type reactor inlet and the feed point of the intermediate steam injection to SI type reactor, respectively. The values of the bounds to these variables have been set at the maximum values possible. The additional variables used for the DB reactor involves the diameter (D_2) of the second bed of the reactor and the $(L/D)_2$ ratio for the second bed reactor length. The ranges of these two decision variables have been set following the range of the diameter and L/D ratio of the first bed. The reactor intermediate temperature (T_{mix2}) is selected to provide sufficient thermal boosting to the reaction process.

Variables T_{C1}, T_{mix1} and T_{mix2} (for SI reactor only) are calculated by performing energy balance and assuming negligible heat loss in the mixers. The optimization problem solved is subject to the following constraints:

$$650 < T_{\text{mix1}} < 925\,\text{K}, \tag{30}$$

$$650 < T_{\text{mix2}} < 925\,\text{K} \quad \text{(for SI reactor only)}, \tag{31}$$

$$P_{\text{exit}} > 1.4\,\text{bar}, \tag{32}$$

$$T_{H1} - T_{C2} \geqslant 10\,\text{K}, \tag{33}$$

$$T_{H2} - T_{C1} \geqslant 10\,\text{K}, \tag{34}$$

$$F^0_{EB} \times SOR \leqslant 453.59\,\text{kmol/h} \tag{35}$$

where T_{mix1} is the temperature of EB and superheated steam mixture at the reactor 1 inlet and T_{mix2} is the temperature of the products of reactor 1 and superheated steam mixture at the reactor 2 inlet. The constraints on T_{mix1} and T_{mix2} are based on the minimum temperature required for reaction to occur and the temperature at which catalyst starts to deactivate (Clough and Ramirez, 1976). The reactor exit pressure, P_{exit} should be greater than 1 bar to avoid reactor and other equipments operating under vacuum. Considering pressure drop in the downstream heat exchanger, the lower limit on exit pressure is set at 1.4 bar. The purpose of the two constraints (Eqs. (33) and (34)) is to ensure a 10 K driving force in the heat exchanger.

5. Results and discussion

Optimization study of the industrial manufacturing process of SM has been carried out with real parameter NSGA-II. The design and operating values of the process models are taken from published industrial data (Sheel and Crowe, 1969; Elnashaie and Elshishini, 1994). Values of the catalyst properties such as bulk density, particle diameter, etc. were used as constants whereas values of the variables like reactor dimensions and inlet fluid composition and state were used as the basis for deciding the decision variable ranges. In the first part of the optimization study, where only the styrene reactor—EB pre-heater is considered as the process, the inlet ethyl benzene flow (F^0_{EB}) includes styrene, benzene and toluene as impurities with flow rates of 0.67, 0.11 and 0.88 kmol/h, respectively, as obtained from the industrial data (Yee et al., 2003). In the second part, on the other hand, where a wider section of the plant including product cooler, partial condenser and separation units have been considered, the separation process determines the impurities in the EB flow. Temperatures of the saturated steam and the superheated steam were taken at 405 and 1025 K, respectively.

For all the case studies, results were obtained after 100 generations with 80 chromosomes in the population set, using a program based on the NSGA-II code downloaded from IIT Kanpur website (www.iitk.ac.in/kangal/soft.htm) on July 2002. The code provides options for performing an optimization study either with the real-coded operators or with the binary operators. For the present study, we had chosen the

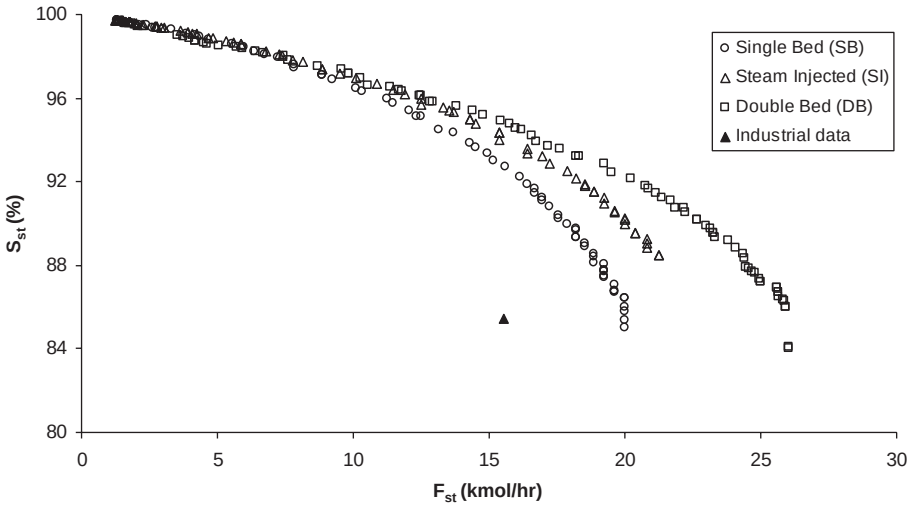

Fig. 3. Pareto optimal set obtained from the simultaneous maximization of styrene flow rate and styrene selectivity.

former as it converged faster in some cases and could produce better Paretos than the binary-code NSGA-II. A more detailed report of this comparative performance analysis can be found in one of our recent publications (Tarafder et al., 2003). The program requires a set of parameters to carry out the study. Like any GA based algorithm, it needs a seed for random number generations (R_s), to start with, and crossover probability (p_c) and mutation probability (p_m), to decide whether the crossover and the mutation operations would be performed or not. Besides, real-coded NSGA-II needs values of the distribution indices for simulated crossover operation (η_c) and simulated mutation operation (η_m). They are used to define probability distributions, which ultimately determine the location of resultant or child solution with respect to the parent solutions (Deb and Agrawal, 1995). For the present study, we used: $R_s = 0.857$, $p_c = 0.7$, $p_m = 0.05$, $\eta_c = 10$ and $\eta_m = 20$, which were obtained after experimentation with a range of values, to generate the best Pareto. NSGA-II uses a tournament selection based, constrained non-dominated sorting method for constraint handling. The process is very efficient and better than the penalty function based methods, which we used in our earlier study (Yee et al., 2003). Average computational time taken for all the optimization studies in this work, i.e. for all the reactor types and for the reactor computation as well as computation for entire manufacturing system, was $\sim$ 6 min. in a 2.4 GHz P4 computer with 512 MB of SDRAM.

5.1. Optimization of styrene reactor—EB preheater unit

Styrene reactor—EB pre-heater unit was first optimized for maximizing the styrene flow rate and selectivity (case 1). The Pareto optimal solutions, for the three different reactor bed designs (Fig. 3), clearly show that the performance of double bed (DB) reactor is the best, followed by the steam-injected (SI) and the SB reactors respectively. Although towards very high selectivity (above 96%) the styrene flow rates are similar for the three reactor types, the difference in F_{st} increases significantly at lower S_{st}. The highest F_{st} generated by the double-bed reactor is $\sim$ 6 kmol/h greater than its single-bed counterpart at the same S_{st}.

Figs. 4 and 5 show the values of the decision variables corresponding to every point of the Pareto sets in Fig. 3, plotted against F_{st}. All the decision variables directly or indirectly contribute to a set of general factors, which actually controls the reactor performance. These factors are: the EB and steam flow rates to the reactor, reaction temperature and pressure, reactor dimension and the catalyst performance. In different combinations, these factors decide EB conversion and styrene selectivity during the reaction process. The role of EB and the steam flow rate is supportive to maximizing both the objectives, F_{st} and S_{st}. This is obvious, as the most important precondition for generating high F_{st} and S_{st} is an availability of high EB flow rate. The same can be said of the steam flow rate, with all its contribution to the reaction discussed before. The role of the reactor temperature, on the other hand, is different for the two objectives. While a high reactor temperature facilitates higher EB conversion, and hence higher styrene flow rate, but at the same time it decreases the styrene selectivity. A low reaction pressure increases the EB conversion and the styrene selectivity simultaneously. The effect of the reactor dimensions on the objectives is not monotonic; it reaches an extremum after which it starts behaving in an opposite way. A high reactor diameter, which lowers the space velocity, increases conversion as well as the S_{st}, if the reactor inlet temperature is kept unaltered. But, a diameter value higher than a critical one increases the reverse reaction and production of by-products thus reduces the performance. On the other hand, if the reactor diameter is lowered, it increases the space velocity and requires a higher inlet temperature to retain the EB conversion rate. So, the reactor diameter can be a factor

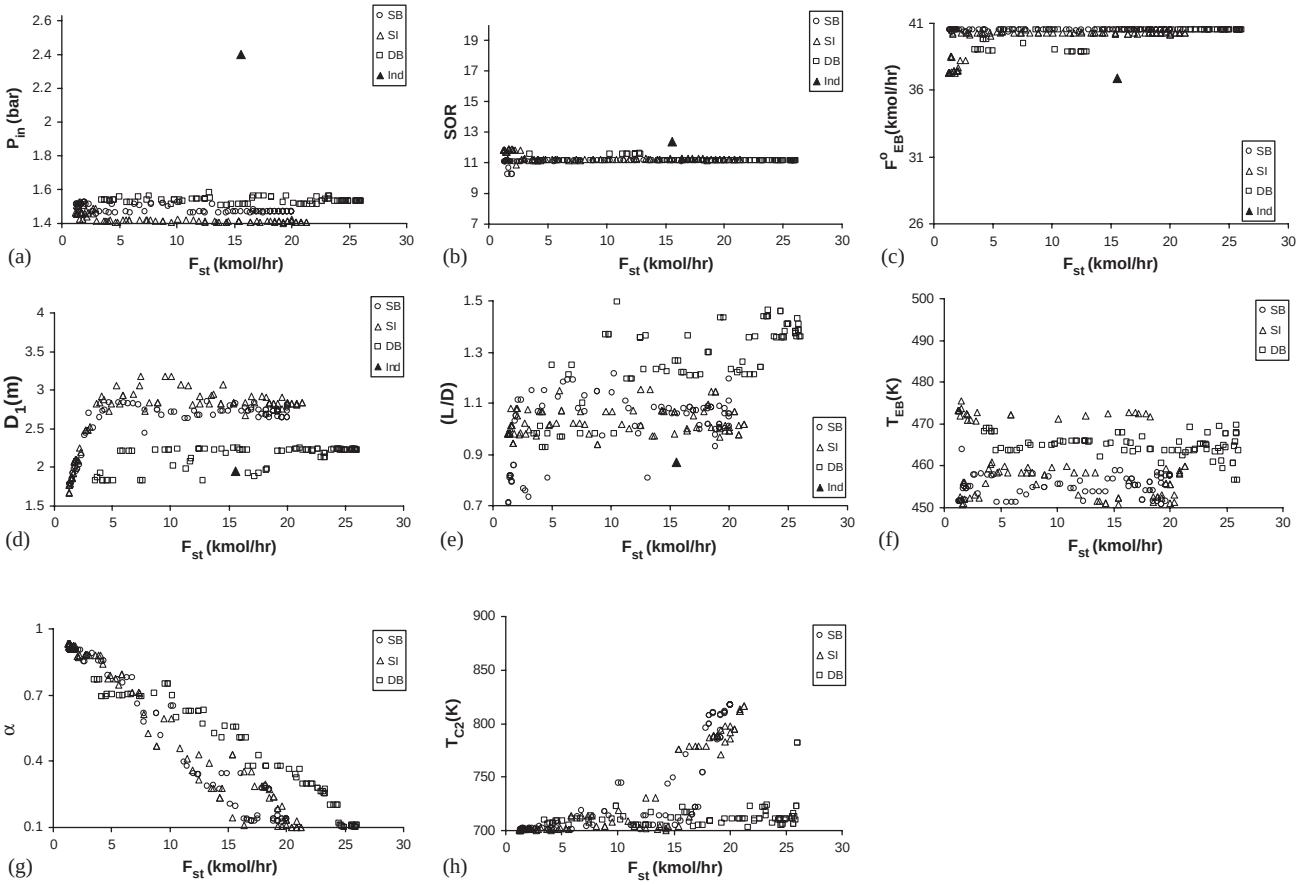

Fig. 4. (a)–(h) Decision variables corresponding to the pareto optimal set in Fig. 3. SB—single bed; SI—steam-fed; DB–double bed; Ind—industrial data.

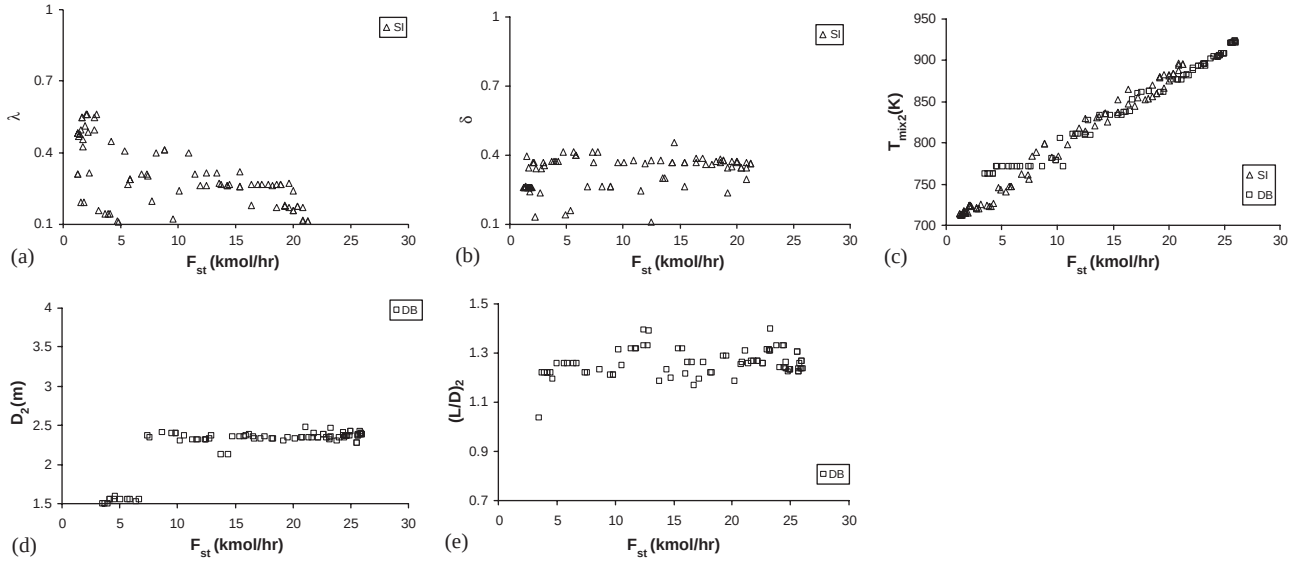

Fig. 5. (a)–(e) Additional decision variables for SI and DB reactors corresponding to the pareto set in Fig. 3. SI—steam-injected; DB—double bed.

for controlling the F_{st} and S_{st} to some extent, when the reactor temperature is kept invariant. The length of the reactor, for a given reactor diameter, determines the total residence time of the reactant–product mixture. While smaller reactor length leads to unfinished reaction with low EB conversion and styrene production, a larger length decreases the selec-

tivity through reverse reaction and by-product generation. The catalyst performance is taken as uniform in the present study and hence it is not considered as a variable. Industrially, to compensate the losses in catalyst activity, the inlet temperature to the reactor must be increased (Lee and Hubbell, 1982).

After identifying the role of the contributing factors in determining the reactor performance, it is required to identify their relations with the decision variables, so that a general estimate regarding the results of the decision variables can be made. A glance at the list shows that the following decision variables—inlet pressure, SOR, EB flow, reactor diameter and reactor length, are the set of factors, which directly control the reaction. The other decision variables, on the other hand, have a combined effect on the reaction temperature, the most important factor that controls the reaction process. An approximate estimate can be made out of this relation that as the Pareto fronts generated by all the reactor types vary smoothly with the F_{st}, the factors which are directly used as decision variables vary smoothly with the F_{st} as well. It can be envisaged that the decision variables whose combined effect determines the reaction temperature may scatter as more than one combination of these variables (degrees of freedom) can create the same thermal effect inside the reactor. We can see from Figs. 4a–c that the values of the inlet pressure, SOR and EB flow are almost invariant with respect to F_{st}, as perceived by the general understanding of the reaction process. On the other hand, values of the decision variables which are related to the reactor temperature, i.e. the EB pre-heater outlet temperature (T_{C2}), the reactor length fraction (λ) and superheated steam fraction (δ for SI reactor), the saturated steam fraction (α) and the reactor intermediate temperature (T_{mix2} for DB reactor)—all display noticeable variation and scatter with respect to the F_{st}. Scattering of similar magnitude was noted even when tried with different values of NSGA-II parameters, and even with other optimization routines (Tarafder et al., 2003). As we have discussed elsewhere (Tarafder et al., 2004), that scatterings of decision variables increase with the increase in the degrees of freedom (decision variables), and a systematic approach should be devised to lessen it. This may drastically increase the acceptability of the multi-objective optimization results to the plant operators and designers, by offering more acceptable and achievable choices.

The decision variables related to the reactor dimension, i.e. the reactor diameter(s) (Figs. 4d and 5d) and length(s) (Figs. 4e and 5e), although scattered, have an overall trend to reach uniformity. The trend of the temperature related decision variable values is expected as it affects the F_{st} and S_{st} in opposite way and the reason for the scattering can be understood from the previous argument. The scatter in the reactor dimension decision variables, on the other hand, is related to the scatter in the temperature related decision variables, as both the factors, the reactor diameter as well as the temperature, can independently affect a change in the F_{st} and S_{st}. If closely scrutinized, it can be seen that any change in the reactor diameter has been reciprocated by a change in the reactor temperature.

A comparative analysis between the decision variables of different reactor types is necessary to understand the reasons behind their performance difference. Before going further into the comparative analysis, note that in all the figures representing the decision variables (Figs. 4 and 5), changes in decision variables up to F_{st} equal to 10 kmol/h are very random in general. This is possibly because up to this point the overall conversion of EB is lower than 20% (Fig. 6c) and it is expected that a wide range of decision variable combinations can result in such meager conversion leading to this general scattering. In the remaining part, any trend of decision variables below this F_{st} mark would not be discussed to avoid repetition of similar arguments.

Starting with the reactor inlet pressure, it can be observed that the values are mostly invariant and are close to 1.4 bar, the minimum pressure constraint. It can be also observed that the DB reactor requires the maximum pressure followed by the SB and the steam injected respectively. It is expected, as the DB with shorter reactor diameters (Figs. 4d and 5d) and longer reactor lengths (Figs. 4e and 5e) offers the maximum resistance to flow, whereas the steam injected offers least resistance as only a portion (Fig. 5b) of the total throughput covers the entire reactor length. For the EB and the steam flow rates, it can be seen that all the decision variable values are almost equal to the highest possible, bound by their upper limits (40.56 kmol/h for EB) and steam flow constraint (453.59 kmol/h), respectively. An abrupt variation of few EB flow points representing the DB reactor can be noted. A close observation shows that the lower EB flow is compensated by a combined effect of a sudden rise in the reactor temperatures (Figs. 6a and 6b) and the reactor diameters (Figs. 4d and 5d) to produce a smooth Pareto. In a later part it will be shown that with compensation from reactor temperature and reactor diameter, a far lower EB flow rate is sufficient to generate similar F_{st}–S_{st} Pareto as in Fig. 3 up to moderately high F_{st}. However, to produce very high F_{st}, maximum possible EB flow is absolutely necessary.

The effect of all the temperature related decision variables are combined into the reactor inlet temperature (Fig. 6a) and the reactor intermediate temperature (Fig. 5c). It can be seen that whatever way the contributing decision variables might have varied, both the temperatures increase almost monotonically towards higher F_{st}, as required by the reaction chemistry. Towards lower F_{st}, however, the reactor diameter controlled the performance and temperatures did not vary. The reactor inlet temperature (T_{mix1}) is controlled by the pre-heater exit temperature (T_{C2}) and the superheated steam flow rate $[(1-\alpha)\delta F^0_{stm}]$ at the reactor inlet. Values of the pre-heater exit temperature (Fig. 4h) vary close to the lower bound except for the SB and SI type where the values changed suddenly towards higher F_{st}. Reason for the generally low pre-heater temperature is the constraint (Eq. (33)) that the reactor outlet temperature (see Fig. 6b) should be at least 10 K higher than the pre-heater outlet

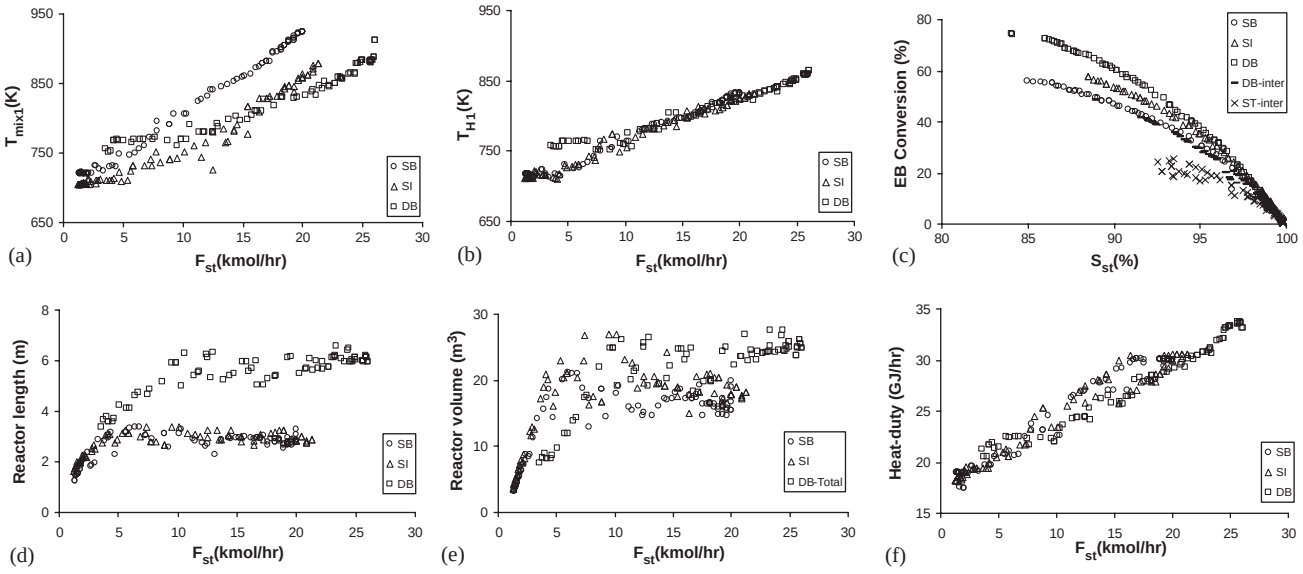

Fig. 6. (a)–(f) Calculated values of some variables corresponding to the pareto set in Fig. 3. SB—single bed; SI—steam-injected; DB—double bed; DB-inter—outlet to the first bed of DB reactor; SI-inter—SI reactor point just before intermediate steam mixing; DB-total—Adding both the beds of DB reactor.

temperature (T_{C2}). To satisfy this, the optimizer opted for lower pre-heater temperature, so that higher temperature drop, resulting higher conversion across the reactor, can take place. The steady increase of the reactor inlet temperature, on the other hand, is supported by the increasing flow of superheated steam, which is evident from the values of saturated steam fraction (Fig. 4g), decreasing steadily with F_{st}. For the SB and SI reactor, T_{C2} increases towards the end because even maximum superheated steam flow was not sufficient to raise the temperature to the required level to producing high F_{st}. It can be observed that only after the net superheated steam flow to the reactor reached its maximum (indicated by the lowest α values in Fig. 4g), the optimizer started selecting higher T_{C2} values (Fig. 4h). However, with higher pre-heater temperatures, lower superheated steam flows (higher α) were selected again, which gradually increased to reach the maximum F_{st} point of the SI reactor. Similar phenomenoncan be observed for the SB reactor as well. The intermediate temperature of the SI reactor is controlled by the reactor length fraction (λ) (Fig. 5a) and the superheated steam fraction (δ) (Fig. 5b), whereas for the DB reactor, it's the superheated steam flow (at 1025 K) that indirectly heats the outlet flow of the first bed. It can be noticed that the DB intermediate temperatures are higher than the inlet temperatures as the first bed outlet temperatures are higher than the temperatures of the pre-heater outlet flow. For the SI reactor, the λ and δ values were chosen as to boost the reaction temperature at a suitable intermediate point so that increased objective values are achieved. Cross-referring the values of the SI reactor diameter and the inlet and intermediate reactor temperatures can perform an analysis of the pattern of changes in λ and δ. Fig. 5a shows that λ decreases towards higher F_{st} making the second part of the reactor longer and the first part shorter. The reason behind this trend will be addressed later in the analysis of SI reactor dimensions. Fig. 5b shows that the δ value chosen is ~ 0.37 over a wide range of F_{st} values, and this is probably the best way to distribute the steam.

A comparative analysis of the reactor inlet (T_{mix1}) and the intermediate (T_{mix2}) temperatures is necessary to understand the reason behind the performance difference between the different types of reactors. Fig. 6a shows that the inlet temperature of SB reactor is higher than both the SI and DB type. As EB conversion is directly dependent on the reactor temperature and the reaction process decreases the reactor temperature along its length, only a very high inlet temperature for SB reactor can ensure sufficiently high temperature throughout the reactor length to achieve the required conversion. It can be seen from Fig. 6a that the inlet temperature of SB reactor reached the maximum limit to produce the maximum F_{st}. However, in the process of increasing the F_{st}, it has to largely compromise with the S_{st}, and made its overall performance worse than the other reactor types. On the other hand, for both the SI and DB type reactors there are intermediate supplies of energy to boost the reactor temperatures and so its inlet temperatures are not chosen as high as that of SB. Obviously this was done to keep the S_{st} values high for them.

The diameter selection of all types of reactors is very much dependent on their temperature selection. It can be observed that although almost uniform diameter is selected by all the reactor types at the highest respective F_{st}, significant scattering is there in between. The diameters at the respective highest F_{st} may be the best for the reactor inlet or intermediate temperatures having upper limit at 925 K. A comparative observation of the entire range of values of

the reactor diameters (Figs. 4d and 5d) and reactor inlet and intermediate temperatures (Figs. 6a and 5c) shows that all the values are often abruptly, but complementarily chosen to maintain a smooth Pareto of the objective values. However, most distinctively, the DB type reactor has chosen much lower diameters than its counterparts. Starting with the SB reactor, it is understandable that an absence of any intermediate heating has forced it to maintain a high reactor diameter, as well as high reactor inlet temperature to maximize the F_{st}, by maximizing EB conversion. At lower inlet temperatures it could retain high S_{st} value comparable to other reactors, however, as the inlet temperature is increased, S_{st} decreased sharply. The final diameter chosen by the SB reactor is probably the best to produce the highest F_{st} with the minimum sacrifice in the S_{st}. The DB reactor, on the other hand, has the option of distributing the reaction process in two separate beds to maximize the objectives. The lower reactor diameter (Fig. 4d) and lower inlet temperature (Fig. 4h) chosen by the DB for its first bed is to convert the EB, keeping the S_{st} as high as possible (Fig. 6c). The second bed, however, converts the EB aggressively to maximize the F_{st}, which is evident from the high inlet temperature (Fig. 5c) and higher diameter (Fig. 5d) of the second bed. This reduces the S_{st} values significantly in the second bed, but the overall S_{st} can be maintained high enough taking the F_{st} value far higher than other two reactors (Fig. 3). Anobvious comparison comes between the performances of the DB reactor and the SI reactor, as the operational strategy of SI is very close to the former type. Figs. 6a and 5c show that both the inlet (T_{mix1}) and intermediate (T_{mix2}) temperatures of SI reactor can be higher than the DB type, along with that, the optimizer could have chosen any reactor dimensions to make the SI reactor performance comparable to that of DB. But this could not happen, as the real difference in their performance is made in the first part of the SI reactor. The first part, having less than half the volume of the total steam, results in much higher partial pressures of the reactants compared to the first bed of DB. This high reaction pressure significantly reduces the EB conversion in the first bed (Fig. 6c) even at high temperatures and large diameters. It can be seen that the initial conversion as well as the initial F_{st} from the first part of SI reactor is far lower than the DB first bed outlet. Though the second part of SI shows a comparable, even better, performance than the second bed of DB, the overall performance could not be matched. The higher reactor diameter chosen by SI is to boost the low EB conversion in the first part. Regarding the reactor lengths, although L/D ratios show lots of scattering, the actual reactor lengths (Fig. 6d) are well defined. Fig. 6d shows that the total length of both the SB and SI type reactors reach a uniform value circa 3 m, while the length of the DB type increases with the F_{st} with values almost twice as the other types. To keep the total reactor volume comparable, the total reactor length of DB is chosen higher than the other two types, as diameters of both the DB reactor beds are lower than the others. It can be observed that the reactor length of DB increases towards the highest F_{st}. This is to increase the total reactor volume, for more EB conversion, keeping the diameters fixed. The decreasing value of λ in SI reactor can be explained with similar argument. As the performance of the first part of SI reactor could not be better, the optimizer increased the length of the second part to boost the performance to the maximum achievable level. Selection of the EB inlet temperature (Fig. 4f) by the optimizer is influenced by the pre-heater temperature difference constraints (Eqs. (33) and (34)), values of the saturated steam fraction (Fig. 4g) and the pre-heater outlet temperature(Fig. 4h). In the optimization study, it has little role in evaluation of the objectives.

The optimization results bring out some revealing facts regarding the reactor volume and the heat duty required by the reactors. Intuitively, it may look that the total reactor volume of DB type must be much higher than the other two types and the heat duty required by it should be far higher. But from Fig. 6e it is clear that the total reactor volume of DB is comparable to the other types and the heat duty (Fig. 6f) required, in actuality, is marginally lower than the SB type and almost equal to the SI type reactor. The total volume is comparable as the diameters of both the beds were chosen far lower than the other types. Regarding the heat duty, it can be seen from Fig. 4g, that the total steam-flow for superheating in DB is far lower than the others and for this reason the total heat carried by the steam to DB reactor is the same or even lower.

The styrene flow and styrene selectivity were chosen as the objectives of this optimization study as these are the main factors of the styrene reactor which ensures maximum styrene production. The results generated by the optimization, however, show that a bi-objective optimization of F_{st} and S_{st} computes the maximum possible F_{st} values, but it does not ensure the maximum profitable situation. For example, even to produce low styrene flows (at high S_{st}), the optimizer had chosen highest possible EB flow and the other contributing factors accordingly. We have argued earlier that far lesser EB flow rates could have been chosen at this situation, along with appropriate reactor dimensions and temperatures. As this lowers plant running cost, this may create a big difference in the plant economics. In industries unreacted EB is recycled to the process, but the separation of un-reacted EB from styrene is very costly. So, usage of minimal EB flow or maximum conversion of EB ensures lower operating cost. This fact leaves space for a look into the EB conversion aspect as well. It was perceived that the performance of the SM reactor cannot be fully understood unless it is optimized along with the conversion of EB as well.

The DB type reactor was chosen for a tri-objective optimization study by maximizing the F_{st}, S_{st} and EB conversion (case 2). The results generated by this study were compared to the bi-objective optimization results of DB reactor. Fig. 7 plots EB conversion as well as S_{st} against F_{st} for both the bi- and tri-objective optimization study. The figure shows that the F_{st}–S_{st} trade-off is better in the bi-objective

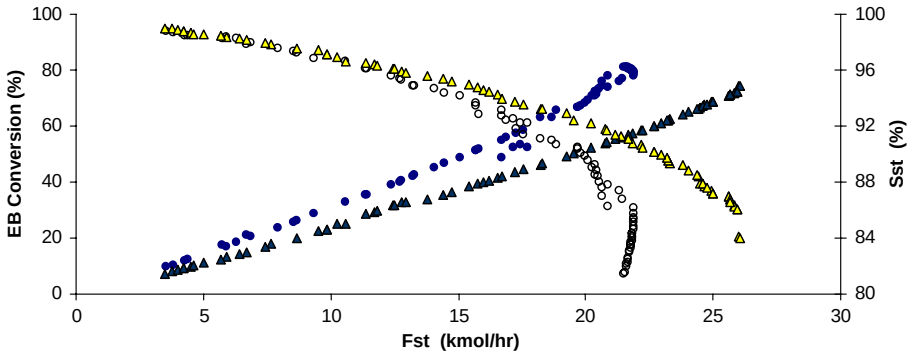

Fig. 7. Comparison of the performances of DB type reactor plotted as (a) F_{st} versus EB conversion and (b) F_{st} versus S_{st}, from (1) Pareto obtained from tri-objective optimization of F_{st}, S_{st} and EB conversion [(●) for (a) and (○) for (b)]; and (2) bi-objective optimization of F_{st} and S_{st} [(▲) for (a) and (△) for (b)].

study than the tri-objective; particularly at high F_{st} values. However, corresponding EB conversion of the bi-objective process is much lower than that suggested by the tri-objective process. Higher conversion means handling lower volume of un-reacted EB in the EB–styrene separation unit, resulting in lower steam cost for the distillation column reboiler. On the other hand, lower selectivity means higher conversion of EB to benzene and toluene, and as the market price of both the benzene and toluene is lower than EB, lower selectivity means raw material degradation. A comparison of the benefits from the above schemes can be made. It should be noted that the amount of heat duty required in the EB–styrene separator is significantly high because of high latent heat of EB and the close boiling points of styrene and EB, requiring high reflux ratio. If the price of toluene and benzene is much lower than EB, selectivity should be the main criterion for selecting a suitable operating point. On the other hand, if toluene and benzene price comes closer to the EB price but steam cost is on the higher side, conversion of EB should be taken into foremost consideration. Another basis of comparison is the styrene price. If the styrene price rises significantly, then the objective should focus on production of the highest styrene possible, even at the cost of lower selectivity or lower conversion. As the international market price of styrene varies widely, this type of comparison carries useful insight. From a comparative study of these results (Fig. 7), it can also be said that under the stated operational limitations, if the required selectivity is greater than 93%, the decision variables suggested by the tri-objective optimization process is more economical. For a requirement of maximum F_{st} within the operational limits, however, the variables suggested by bi-objective optimization process are better.

A comparison of decision variables of the DB reactor, generated through bi- and tri-objective optimization (Fig. 8), brings out the reason for the difference in their respective performances. It can be seen from Fig. 8b that much lower EB flow is required for tri-objective case, accompanied by an elevated SOR (Fig. 8a) as well as reactor intermediate temperature (T_{mix2}) (Fig. 8d). The reactor diameter of the first bed (Fig. 8c), on the other hand, is higher for the tri-objective case. The higher inlet temperature and higher diameter requirement for the tri-objective case is understandable as both these factors lead to high EB conversion. As role of the other decision variables has been already discussed and as they don't change significantly in the tri-objective case, no further discussion of the other decision variables is made.

5.2. Optimization of styrene manufacturing process

From the study of the styrene reactor-EB pre-heater optimization, it was evident that conversion of EB is a crucial factor in the reaction, affecting the required heat duty while separating the downstream components. For studying the effect of the reaction process on the heat requirement at the separation units, the next phase of the study includes the cooling as well as the separation units along with the reactor unit. The main source of energy for the reaction and for the distillation is saturated as well as superheated steam. The study on the entire manufacturing process focuses on reduction of total steam (heat duty) used along with the increase in styrene flow rate and selectivity. The study is carried out only on the DB type reactor as this has been identified as the best reactor configuration in the previous section.

Fig. 9 plots the Pareto optimal set of the tri-objective optimization of styrene manufacturing process for maximization of F_{st} and S_{st} and minimization of the total heat duty (Q) required (case 3). The results are plotted as S_{st} and Q against F_{st}. The F_{st} vs. S_{st} Pareto optimal set of the bi-objective optimization of DB reactor (case 1) has also been plotted on the same figure for comparison. Although Fig. 9 shows that the F_{st}–S_{st} Pareto optimal set of the tri-objective optimization problem is scattered and performing worse than the F_{st}–S_{st} set of bi-objective one, this compromise was made to minimize the total heat duty requirement of the entire plant. In the bi-objective optimization section, a general analysis of the decision variables and their effects on the F_{st} and the S_{st} values has already been done. This section requires a general understanding of the third objective, the heat duty (Q) minimization. The heat duty requirement to

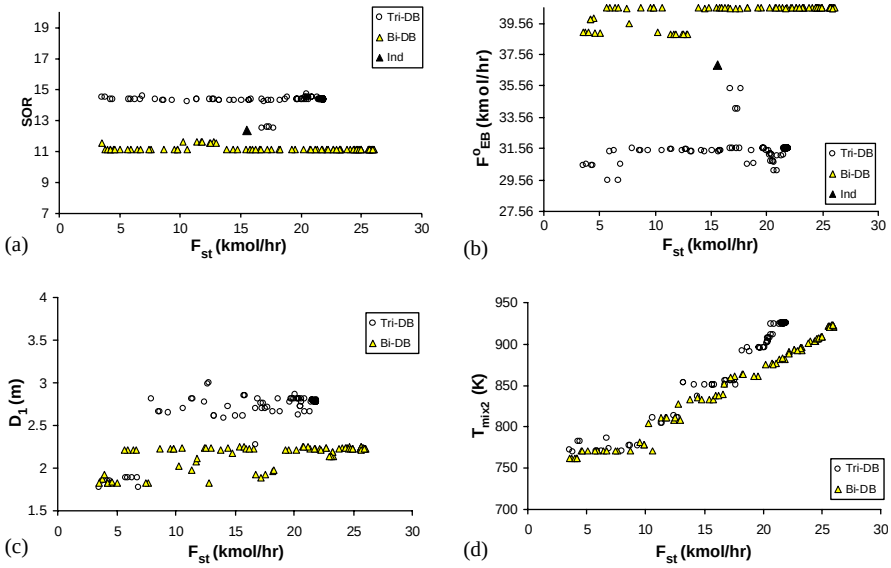

Fig. 8. (a)–(d) Some decision variables corresponding to the pareto sets referred in Fig. 7. Tri–DB—results from tri-objective and Bi-DB–results from bi-objective optimization of double bed reactor; Ind—Industrial data.

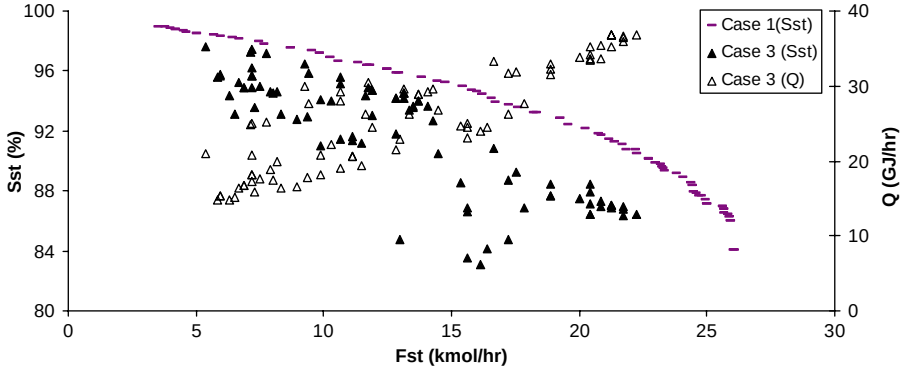

Fig. 9. Comparison of the performance of: Case 1—bi-objective optimization of F_{st} and S_{st}; and Case 3—tri-objective optimization of F_{st}, S_{st} and heat duty (Q). [-]: pareto set of F_{st} vs. S_{st}; [▲] F_{st} vs. S_{st} plot; [△] F_{st} vs. heat duty (Q).

a styrene manufacturing process can be divided under two major heads. One part, which is calculated here by the SOR and the EB flow rate, enters the reactor as saturated or superheated steam, pre-heats and inter-heats the EB feed, ultimately fed to the reactor as a reactant to the process. The other part, on the other hand, is used as an indirect supplier of heat to the reboiler units of the distillation columns. If lesser steam is supplied to the reactor, resulting in un-reacted EB, the reboiler heat duty at the EB–styrene separation unit will increase drastically to separate the increased un-reacted EB. The process will act vice-versa. Thus the total heat duty minimization (duty to the reactor plus duty to the separation units) acts counteractively in generating the best set of results. From this observation, it can be predicted that the minimization attempt of the total heat duty in the process may generate scattered objectives because of the counteracting effects.

The inlet pressure, P_{in}, selected by tri-objective optimization study is slightly higher than the bi-objective one; although it likely maintained the lowest pressure possible satisfying all other constraints. The main reason for choosing slightly higher pressure is because of the lower reactor diameter, which will be discussed later. Both the SOR (Fig. 10a) and the EB flow rate (Fig. 10b) of the tri-objective optimization study is scattered in nature. This was speculated, for the counteracting effect of the heat duty (Q) minimization objective on the reactor steam flow rate. The EB flow rate is also scattered for another counteracting effect. In the bi-objective optimization study, we have seen that the F_{st} and the S_{st} maximization requires the highest possible EB flow. On the other hand, the heat duty minimization, which requires minimum handling of un-reacted EB in the separation unit, will try to ensure the minimum required EB flow to the reactor. For these counteracting requirements, the EB flow rates chosen are scattered in nature as well. A plot of the total flow (EB plus saturated and superheated steam) shows that the total flow of the tri-objective optimization study is far lower than that of the bi-objective (Fig. 11a).

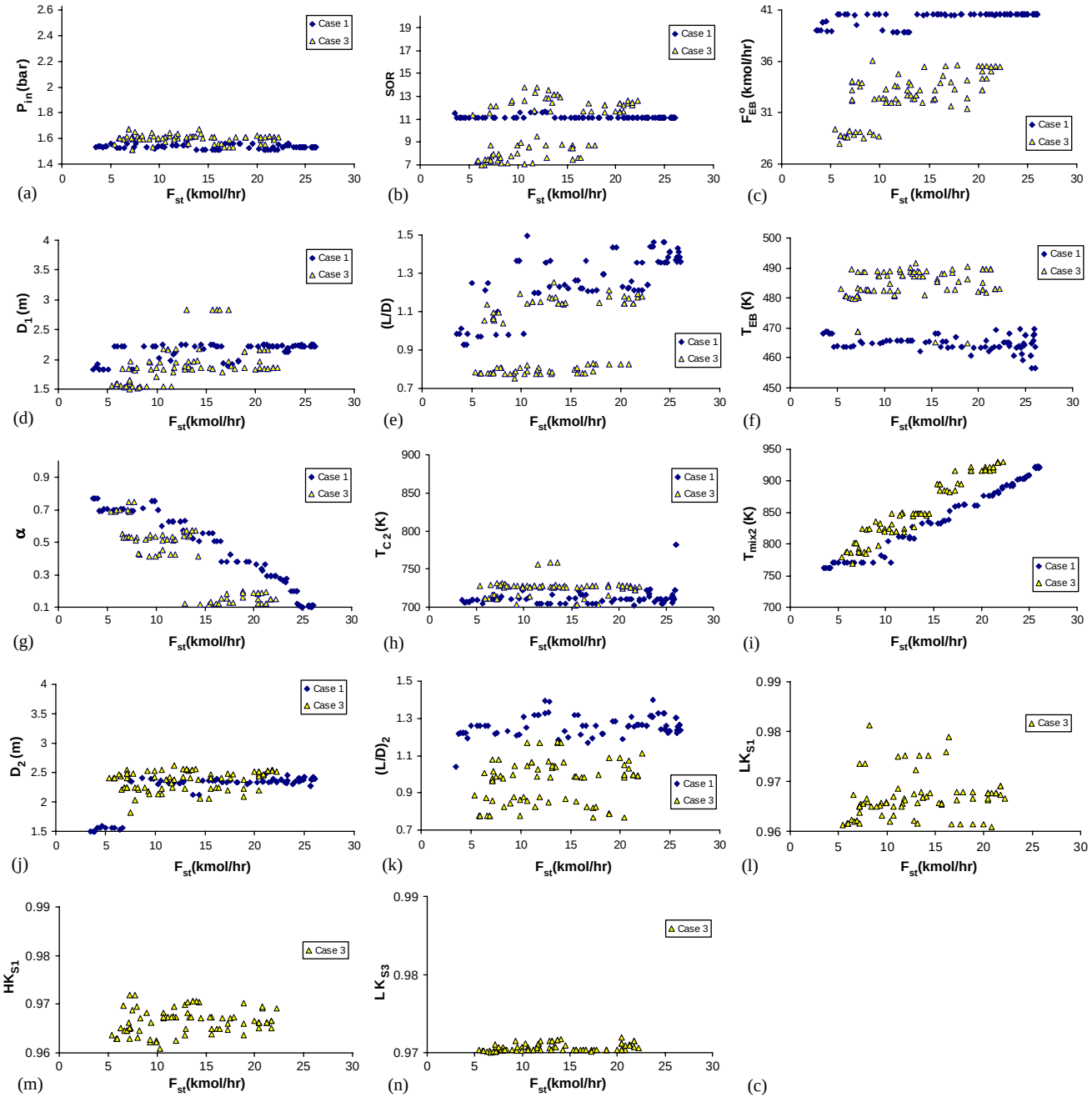

Fig. 10. (a)–(n) Decision variables corresponding to the bi- and tri-objective optimization referred in Fig. 9. Case 1—results from double-bed bi-objective optimization of F_{st} and S_{st}; Case 3—results from double-bed tri-objective optimization of F_{st}, S_{st} and heat duty.

Figs. 11b and 10g show that both the inlet (T_{mix1}) as well as the intermediate (T_{mix2}) temperatures from tri-objective optimization, are higher than their bi-objective counterparts. These selections were aimed at increasing the EB conversion in the reactor so that F_{st} is maximized as well as minimizing un-reacted EB moving to the separator. The two contributing decision variables to the values of T_{mix1} and T_{mix2}, the saturated steam fraction (α) and the pre-heater outlet temperature (T_{C2}); both these support increment of T_{mix1} and T_{mix2} (Figs. 10e and f). The values for both the decision variables have been chosen to ensure higher heat flow than their bi-objective counterparts. Although the fraction of superheated steam flow is higher for tri-objective case (lower α see Fig. 10e), the overall heat duty supplied to the reaction process (Fig. 11c) is still lower due to lower EB flow and SOR.

The reactor diameters chosen by the tri-objective study for its first bed is almost half as those chosen by the bi-objective (Fig. 10c), whereas for the second bed (Fig. 10h), the values are comparable, even higher at certain points. While discussing the bi-objective results, we have analysed the reason

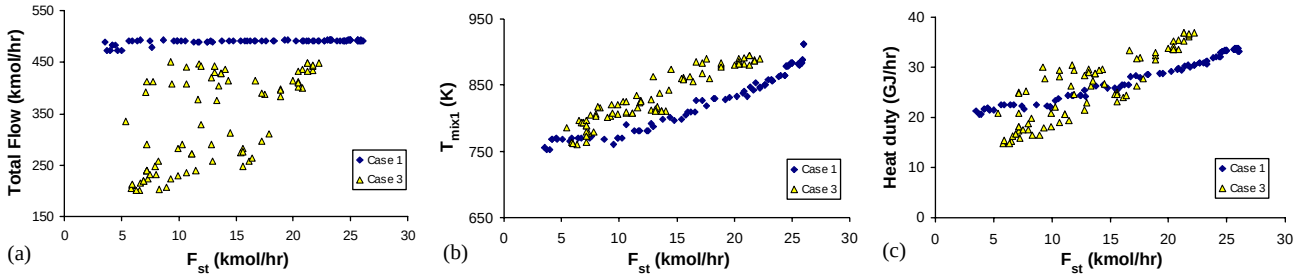

Fig. 11. (a)–(c) Calculated values of some variables corresponding to the bi- and tri-objective optimization referred in Fig. 9. In Fig. 11c, Case 1 comprises heat-duty to the reactor only, whereas Case 3 comprises heat-duty to the reactor as well as the separation unit reboilers. Case 1—results from double-bed bi-objective optimization of F_{st} and S_{st}; Case 3—results from DB tri-objective optimization of F_{st}, S_{st} and heat duty (Q). Note: In Fig. 11c, the heat duty referred to Case 1 is for the reactor unit only, whereas for Case 3 it's for the entire manufacturing process.

behind the choice of lower reactor diameters. The first bed diameter was chosen lower to keep the S_{st} high while trying to increase the EB conversion. Tri-objective optimization has chosen still smaller diameters because of higher inlet temperatures than the bi-objective. Additionally, the low total flow rate handled by the tri-objective case makes the diameter still lower. For the second bed, however, in an attempt to attain the highest F_{st} the diameters are made higher to maximize the EB conversion. The lengths of both the reactor beds (Figs. 10d and i) are chosen lower than their bi-objective counterparts as the tri-objective study handles lower total flow of EB and steam.

An analysis of the three more decision variables used in the tri-objective study shows that the first two variables, the light key and the heavy key fractions of the first distillation column have selected moderate values (Figs. 10j and k). This shows that the optimizer tried to push more EB in with the benzene-toluene flow and more benzene with the EB–styrene flow. This attempt, most likely, was made to decrease the total flow rate of EB to the reactor by replacing it with toluene impurities. Values of the last decision variable, the light key fraction at the EB–styrene column (Fig. 10l) also shows similar trend, where maximum impurities were tried to mix with the EB flow to keep the heat-load lower at the condenser.

6. Conclusions

A multiobjective optimization study of an industrial styrene reactor unit as well as the entire styrene manufacturing process was carried out with elitist NSGA or NSGA-II. The objectives were to maximize the styrene flow and the styrene selectivity for the first part and styrene flow, styrene selectivity and total heat duty for the second part. Pareto optimal sets were successfully obtained for all the cases. The trend of the decision variables generated could be explained qualitatively, which shows the reliability of the results. In the first part of the optimization study, three variations of styrene reactor were used for a comparative analysis of their respective performances at the optimized condition. It was observed that although at higher selectivity the performances of all the reactor types are comparable, the double bed (DB) reactor is far more efficient than the other types in producing high styrene flow from equivalent EB flow input. The optimization brought out certain facts regarding the reactor volume and the heat duty required by the reactors, which are counter intuitive. Initially it may look that the total reactor volume of DB reactor must be higher than the other two types and the heat duty required by it should be far greater. But it was observed that the total DB reactor volume is comparable to the volumes of other types and the heat duty required is actually lower than the single bed type and almost equal to the steam-injected type reactor. The optimization of the entire styrene manufacturing process suggested different operating points to run the plant at different levels of by-product formation, EB recycle handling and total heat duty minimization.

The optimization routine, NSGA-II, used in the present study proved to be relatively more efficient than the NSGA routine used in our previous study (Yee et al., 2003). With NSGA-II, we could always reach the final solution faster and with a better distributed and wider spread Pareto. It was also noticed that the constraint domination criteria of NSGA-II worked better than the penalty function approach of constraint handling in NSGA, which was used earlier (Yee et al., 2003). While NSGA-II could take all the solutions to the feasible region within first few generations, NSGA generated infeasible solutions till close to the last generation. It was speculated that NSGA couldn't generate a wider Pareto like NSGA-II, because the large dummy values, awarded to the objectives of infeasible solutions, kept nearby potential feasible solutions out of the search space.

Notation

A	surface area, m^2, (also) frequency factor
C	molar concentration, $kmol/m^3$, (also) number of components
c_p	molar heat capacity for hot fluid, kJ/kmol/K

C_p	molar heat capacity for cold fluid, kJ/kmol/K
D	diameter, m, (also) distillate, kmol/h
F	molar flow rate, kmol/h, (also) distillation column feed, kmol/h
H	enthalpy, kJ/kmol
HE1	EB feed pre-heater
HE2	recycled EB heater
J	maximization equation
K	vapour liquid equilibrium constant
L	total length of reactor, m, (also) liquid flow, kmol/h
L/D	reactor length to diameter ratio
m	molar flow rate of hot stream, kmol/h
M	molar flow rate of cold stream, kmol/h
p	partial pressure, (also) probability
P	pressure, bar
Q	rate of heat transfer, kJ/h
R	universal gas constant, 8.314 kJ/kmol/K
R_s	seed for random number
S	selectivity, %, (also) separator
SOR	steam to reactant (ethylbenzene) molar ratio
T	temperature, K
U	overall heat transfer coefficient, kJ/h/m^2/K
V	vapour flow, kmol/h
x	liquid mole fraction
X	conversion, %
y	vapour mole fraction
Y	yield, %

Greek letters

α	saturated steam fraction, (also) relative volatility
δ	superheated steam fraction (only for SI type reactor)
Δ	difference
ΔH	heat of reaction, kJ/kmol
η	distribution index
λ	reactor bed fraction for steam injection (only for SI type reactor)

Superscripts

0	initial
sat	saturated

Subscripts

0	initial
B	boiling point, (also) bottom
bz	benzene
$C1$	cold stream inlet
$C2$	cold stream outlet
CO	carbon monoxide
CO_2	carbon dioxide
c	cross-over
cold	cold stream
cond	condenser
D	distillate
EB	Ethylbenzene
Eth	Ethylene
exit	exit condition
F	feed
Gen	Generation
$H1$	hot stream inlet
$H2$	hot stream inlet
H_2	Hydrogen
hot	hot stream
i	component i, (also) light key component
in	inlet
L	liquid
ln	log-mean
m	mutation, (also) mean
mix1	entry condition at the 1st bed of DB, or 1st part of SI reactor
mix2	entry condition at the 2nd bed of DB, or 2nd part of SI reactor
st	Styrene
stm	Steam
tol	toluene
vap	Vapourization
V	Vapour

Acknowledgements

The authors acknowledge the contribution of Ms Lee Lee Tang Jaimie for writing the initial structure of the simulation program. Special thanks to Prof Kalyanmoy Deb for making the NSGA-II code available on the net (www.iitk.ac.in/kangal/soft.htm).

References

Bhaskar, V., et al., 2000. Applications of multi-objective optimization in chemical engineering. Reviews in Chemical Engineering 16, 1.

Clough, D.E., Ramirez, W.F., 1976. Mathematical modeling and optimization of the dehydrogenation of ethylbenzene to form styrene. A.l.Ch.E. Journal 22, 1097–1105.

Deb, K., 2001. Multi-objective Optimization using Evolutionary Algorithms, Wiley, Chichester, UK.

Deb, K., Agrawal, R.B., 1995. Simulated binary crossover for continuous search space. Complex Systems 9, 115.

Deb, K., et al., 2002. Fast and elitist multiobjective genetic algorithm: NSGA-II. IEEE Transactions of Evolutionary Computing 6, 182–197.

Denis, H.J., Castor, W.M., 1992. In: Elvers, B. et al. (Ed.), "Styrene" in Ullmann's Encyclopedia of Industrial Chemistry, vol. A25. Wiley, New York, pp. 325–335.

Elnashaie, S.S.E.H., Elshishini, S.S., 1994. Modelling, Simulation and Optimization of Industrial Fixed Bed Catalytic Reactors. Gordon and Breach Science Publisher, London, pp. 364–379.

Kasat, R.B., Gupta, S.K., 2003. Multi-objective optimization of an industrial fluidized-bed catalytic cracking unit (FCCU) using genetic algorithm (GA) with the jumping genes operator. Computers and Chemical Engineering 27, 1785–1800.

Khoury, F.M., 1999. Predicting the Performance of Multistage Separation Processes, CRC Press, LLC.

Lee, C.H., Hubbell, O.S., 1982. In: McKettam, J., Wesmantel, G.E. (Eds.), "Styrene" in Encyclopaedia of Chemical Processing and Design, vol. 55. Wiley, New York, pp. 197–217.

Mitra, K., Gopinath, R., 2004. Multiobjective optimization of an industrial grinding operation using elitist nondominated sorting genetic algorithm. Chemical Engineering Science 59, 385–396.

Rajesh, J.K., et al., 2001. Multi-objective optimization of industrial hydrogen plants. Chemical Engineering Science 56, 999.

Saunders, E.A.D., 1988. Heat Exchangers: Selection, Design and Construction. Longman Scientific and Technical, New York, pp. 528–529.

Seider, W.D., et al., 2004. Product and Process Design Principles: Synthesis, Analysis, and Evaluation. Wiley Text Books, 2nd. Wiley, New York, pp. 445–446.

Sheel, J.G.P., Crowe, C.M., 1969. Simulation and optimization of an existing ethylbenzene dehydrogenation reactor. Canadian Journal of Chemical Engineering 47, 183–187.

Srinivas, N., Deb, K., 1995. Multi-objective function optimization using non-dominated sorting genetic algorithms. Evolutionary Computation 2, 221.

Tarafder, A., et al., 2003. Applications of non-dominated sorting genetic algorithms for multiobjective optimization of an industrial styrene reactor. Proceedings of Second International Conference on Computational Intelligence, Robotics and Autonomous Systems (CIRAS 2003), Singapore.

Tarafder, A. et al., 2004. Multi-objective optimization of an industrial ethylene reactor using a non-dominated sorting genetic algorithm. Industrial and Engineering Chemistry Research, revised manuscript submitted to Industrial and Engineering Chemistry Research, 2004.

Yee, A.K.Y., et al., 2003. Multiobjective optimization of an industrial styrene reactor. Computers and Chemical Engineering 27, 111–130.